Photocatalysis

International Edition: DOI: 10.1002/anie.201505802
German Edition: DOI: 10.1002/ange.201505802

Nature-Inspired Environmental "Phosphorylation" Boosts Photocatalytic H_2 Production over Carbon Nitride Nanosheets under Visible-Light Irradiation

Guigao Liu, Tao Wang, Huabin Zhang, Xianguang Meng, Dong Hao, Kun Chang, Peng Li, Tetsuya Kako, and Jinhua Ye**

Abstract: *Inspired by the crucial roles of phosphates in natural photosynthesis, we explored an environmental "phosphorylation" strategy for boosting photocatalytic H_2 production over g-C_3N_4 nanosheets under visible light. As expected, a substantial improvement was observed in the rate of H_2 evolution to 947 $\mu mol\,h^{-1}$, and the apparent quantum yield was as high as 26.1 % at 420 nm. The synergy of enhanced proton reduction and improved hole oxidation is proposed to account for the markedly increased activity. Our findings may provide a promising and facile approach to highly efficient photocatalysis for solar-energy conversion.*

Hydrogen (H_2) production by the use of a photocatalyst and solar energy is an ideal solution to global energy and environmental issues and therefore attracts enormous interest.[1] Unfortunately, the rational design and development of a low-cost, sustainable, and efficient visible-light photocatalyst continues to be a serious challenge in this field. Graphitic carbon nitride (g-C_3N_4), first discovered by Liebig and termed "melon" ($C_6N_9H_3$), with a graphitic π-conjugated stacking structure consisting of tri-*s*-triazine repeating units, has recently emerged as an attractive metal-free photocatalyst because of the well-suited band positions for photocatalytic H_2 production under visible-light.[2] To improve the H_2-evolution activity of g-C_3N_4, numerous modifications of its synthesis have already emerged, including nanostructure design,[2d–f,h–k,3] molecule incorporation,[4] and element doping.[5] In particular, as motivated by the intriguing chemistry of graphene, the preparation of g-C_3N_4 nanosheets has attracted considerable attention, because it has been predicted that the unique properties of such two-dimensional (2D) polymeric semiconductors would be fully exploited in these materials to maximize photocatalytic activity.[2a,d,3a,6] It has been demonstrated that g-C_3N_4 nanosheets with an anisotropic structure can help to guide charge transfer along the in-plane direction to facilitate the separation of electron–hole pairs and subsequent photocatalysis.[2d,e] Moreover, they were reported to possess more favorable band structures for water splitting relative to bulk g-C_3N_4.[2a,d] Despite these pioneering successes, the activity of g-C_3N_4 for photocatalytic H_2 generation is still moderate.

In this study, natural photosynthesis gave us much inspiration to address this issue. In plants, the light-dependent reactions of photosynthesis occur in thylakoid membranes. As the primary components of thylakoid membranes, phosphates (phospholipids) are known to play vital roles in both transferring electrons in electron-transport chains and pumping protons to drive adenosine triphosphate synthesis during the light-dependent reactions.[7] Meanwhile, at the stage of the "dark" reactions of photosynthesis, some phosphates function directly as mediators to participate in carbon fixation and finally convert solar energy into chemical energy in the form of sugars.[7a] This process is known as the Calvin cycle. Hence, we were inspired to explore an environmental "phosphorylation" strategy that could mimic phosphate-involving natural photosynthesis to improve the photocatalytic H_2 production of g-C_3N_4 nanosheets. Remarkably, the optimum addition of a phosphate (K_2HPO_4) to the reaction system boosted the H_2-generation rate to 947 $\mu mol\,h^{-1}$ under visible light, and an extremely high apparent quantum yield (AQY) of 26.1 % was observed at a wavelength of (420 ± 14.5) nm. To the best of our knowledge, this AQY value is the highest reported for a g-C_3N_4-based photocatalyst (see Table S1 in the Supporting Information). As evidenced by (photo)electrocatalytic analysis and theoretical calculations, this significant improvement in H_2 production relies on the synergy of enhanced proton reduction and improved hole oxidation. More importantly, the phosphate was confirmed to indeed play roles resembling those in natural photosynthesis: as a proton pump to facilitate the proton transfer in reaction solutions, and as a mediator that participates directly in proton reduction, thus leading to a Calvin-cycle-like H_2-evolution pathway.

In this study, g-C_3N_4 nanosheets (CN-NS) were prepared by a modified "bottom-up" dicyandiamide-blowing strategy.[8] Bulk g-C_3N_4 (CN) was also prepared as a reference by the direct polymerization of dicyandiamide.[2a,b] In sharp contrast

[*] G. Liu, Dr. T. Wang, Dr. H. Zhang, X. Meng, Dr. D. Hao, Dr. K. Chang, Dr. P. Li, Dr. T. Kako, Prof. J. Ye
Environmental Remediation Materials Unit and
International Center for Materials Nanoarchitectonics (WPI-MANA)
1-1 Namiki, Tsukuba, Ibaraki 305-0044 (Japan)
E-mail: LI.Peng@nims.go.jp
Jinhua.YE@nims.go.jp
G. Liu, X. Meng, Prof. J. Ye
Graduate School of Chemical Science and Engineering
Hokkaido University, Sapporo 060-0814 (Japan)
Prof. J. Ye
TU-NIMS Joint Research Center, School of Materials Science and Engineering, Tianjin University, Tianjin (P. R. China)
and
Collaborative Innovation Center of Chemical Science and Engineering (Tianjin), Tianjin 300072 (P. R. China)

Supporting information for this article is available on the WWW under http://dx.doi.org/10.1002/anie.201505802.

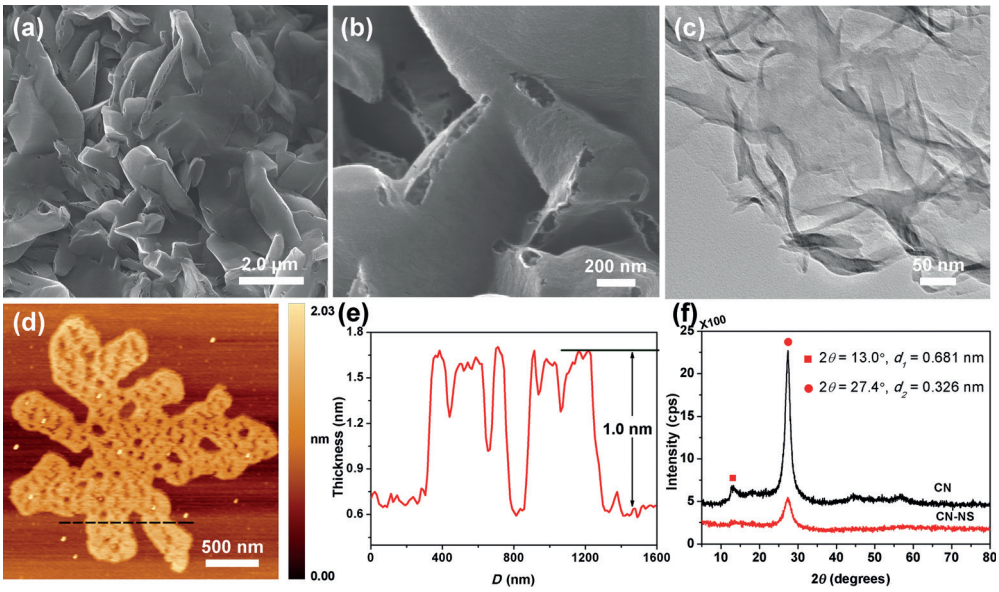

Figure 1. a, b) SEM and c) TEM images of CN-NS. d) Representative DFM image and e) the corresponding height profile determined along the dashed line in (d), revealing a uniform thickness of the g-C_3N_4 nanosheets of about 1.0 nm. f) XRD patterns of CN-NS and bulk CN.

to the dense, stacked lamellar texture of bulk CN (see Figure S1 b in the Supporting Information), CN-NS were shown by scanning electron microscopy (SEM) to be a loose architecture integrated by g-C_3N_4 nanosheets with many wrinkles and irregular holes (Figure 1 a,b; see also Figure S1 a). Transmission electron microscopy (TEM) images further revealed the silklike structure of CN-NS (Figure 1 c; see also Figure S2). Dynamic force microscopy (DFM) of a giant g-C_3N_4 nanosheet indicated that it had a uniform thickness of 1.0 nm, which correspond to about three atomic carbon nitride layers (Figure 1 d,e).[9] X-ray diffraction (XRD) patterns (Figure 1 f) and Fourier transform infrared (FTIR) spectroscopy (see Figure S3 a) demonstrated that CN-NS show the same crystal and chemical structures as bulk CN. From the UV/Vis spectra, CN-NS were found to absorb visible light with a band gap of 2.77 eV (see Figure S3 b).

In a procedure similar to a previously reported method, we examined H_2 production over CN-NS under visible-light irradiation with a Pt cocatalyst and triethanolamine (TEOA) as a hole scavenger.[2b] As expected, CN-NS exhibited superior H_2-evolution activity in comparison with bulk CN (Figure 2 a). This higher activity might be attributed to the higher surface area and the lower electron–hole-recombination rate in CN-NS (see Figure S3 c,d).[4,8] However, the most striking result was that the H_2 evolution was strongly accelerated when K_2HPO_4 (0.20 mol) was added to the CN-NS photocatalytic system. After irradiation for 2 h, the quantity of H_2 gas evolved was about 1.9 mmol, which much exceeds the amount of the catalyst (0.28 mmol). Furthermore, the turnover number (TON) with respect to the number of Pt atoms was calculated to be 247 (please see the Supporting Information for details). These results clearly indicate that the reaction proceeds catalytically.[1a] The influence of the amount of K_2HPO_4 added on H_2 production was further investigated. The optimal amount of K_2HPO_4 in the present photocatalytic system was demonstrated to be 0.20 mol, which led to a H_2-production rate of 947 μmol h^{-1} (ca. 19000 μmol h^{-1} g^{-1}; 50 mg of CN-NS; Figure 2 b). A further increase in the amount of K_2HPO_4 added led to a slight decrease in activity, which may be caused by changes in the pH value of the solution or the surface state of the CN-NS. The details of this effect are still under investigation.

Under the optimal conditions, the wavelength-dependent apparent quantum yield (AQY) of H_2 evolution over CN-NS was shown to distinguish whether the activity was driven by the light-excited electrons in the CN-NS or not. The AQY decreased as the wavelength of the monochromatic light increased, and it qualitatively tracked the characteristic absorption of the CN-NS (Figure 2 c). This result suggests that the H_2 production is primarily induced by the photocatalysis of CN-NS.[2e] At (380 ± 18) nm, CN-NS gave a peak AQY of 45.7 %. Moreover, even under visible-light irradiation at (420 ± 14.5) nm, the AQY still reached 26.1 %, which is much greater than previously reported values (the highest previously reported value is 9.6 %; see Table S1). Comparisons of light absorption, crystal structure, and elemental composition between the as-prepared and the post-reaction CN-NS revealed no obvious change during the photocatalytic reaction (see Figures S5 and S6), thus suggesting good stability of the CN-NS. When methanol or Na_2S was used as the sacrificial agent or the CN-NS catalyst was changed to bulk C_3N_4 or other semiconductors (such as TiO_2, CdS), much improved H_2 yields were also observed after the addition of HPO_4^{2-} (see Figure 2 d and Figure S7), thus confirming the generality of this strategy.

The addition of K_2HPO_4 (0.20 mol) to the normal reaction solution (10 vol % aqueous TEOA) not only led to an increase in the ion concentrations (K^+ and HPO_4^{2-}) but also led to a decrease in the pH value from 10.86 to 10.14 as a result of neutralization between K_2HPO_4 (a typical amphoteric salt, acting as an acid) and TEOA (a typical organic base), both of which have been demonstrated to be critical for the photocatalysis.[10] However, the question still remained as to which factors play the dominant roles in enhancing H_2 production under the present conditions. H_2 production in a pH-adjusted TEOA solution (pH 10.14) was first examined. Although the low pH value was beneficial for proton reduction, slightly decreased activity was observed in comparison with the reaction without K_2HPO_4 (see Figure S8). This result implies that the markedly enhanced H_2 production

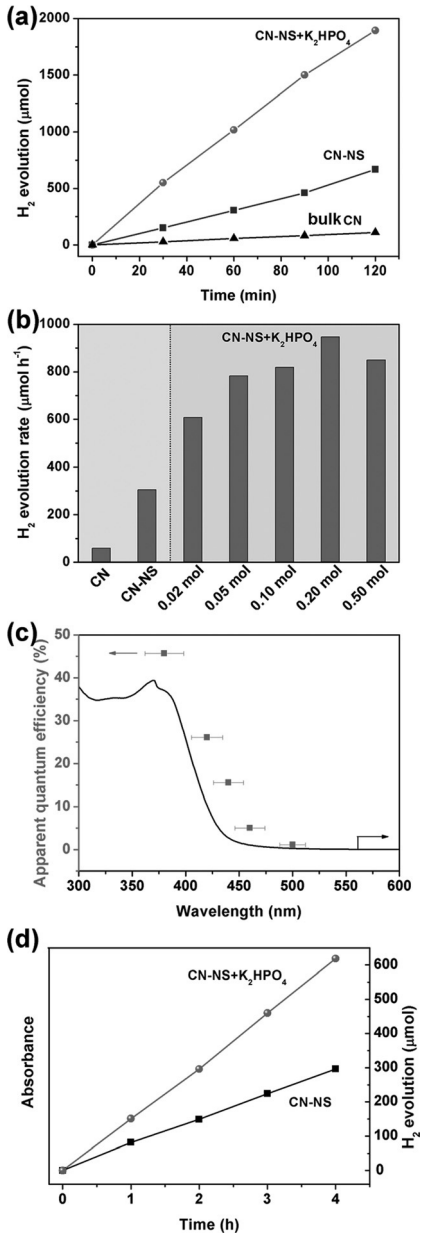

Figure 2. a) H_2 production over CN-NS in aqueous solutions of TEOA. b) Rates of H_2 production from TEOA solutions with different amounts of K_2HPO_4. c) Wavelength-dependent apparent quantum yield (AQY) of H_2 evolution over CN-NS in a TEOA solution containing K_2HPO_4 (0.20 mol). d) H_2-evolution performance in aqueous solutions containing methanol. "CN-NS + K_2HPO_4" in (a, d) indicates that H_2 production was performed in the presence of K_2HPO_4 (0.20 mol). (Light source: 300 W xenon lamp with an L40 cutoff filter.)

cannot be attributed to the decrease in the pH value. We then examined H_2 production in the presence of KCl (0.4 or 0.6 mol). In both cases, very limited enhancement of activity was observed (see Figure S9), thus clearly suggesting a negligible effect of both K^+ ions and the ion strength on H_2 evolution over CN-NS. When the pH value of these KCl-containing solutions was further adjusted to 10.14 with HCl, we were surprised to observe decreased H_2-evolution rates. These combined results indicate that the low pH value adversely affects H_2 production in the present system; it is likely that the oxidative half-reaction of sacrificial agents, as induced by valence-band holes, is suppressed at low pH values.[10c,11] By excluding the effects of the pH value, K^+ ions, and ion strength, we therefore speculate that it is HPO_4^{2-} ions that boost H_2 evolution over CN-NS. Direct evidence to support this conclusion is also the observation that variations in the concentration of HPO_4^{2-} are consistent with the trend in the photocatalytic activity (see Figure S10).

To verify that generated H_2 essentially originates from H_2O rather than HPO_4^{2-}, we conducted isotope tracer analyses with D_2O on a gas chromatograph/mass spectrometer system. Considering the fast H–D exchange of TEOA with D_2O, we used methanol and Na_2S as sacrificial agents in the tests instead of TEOA. Both experiments confirmed the formation of D_2 (see Figure S11). Owing to H–D exchange between D_2O and HPO_4^{2-}, a small quantity of HD was also observed.[12] These results clearly indicate that water is the hydrogen source for H_2 evolution during the above photocatalytic reactions. Because PO_4^{3-} does not contain H^+ but can be converted into HPO_4^{2-} through an ionization equilibrium with H_2O, H_2 production in the presence of K_3PO_4 instead of K_2HPO_4 was also investigated (see Figure S12). As expected, enhanced activity was also observed, which offers additional support to our above conclusion.

Since only slight changes in the pH value of the reaction solution were observed after the addition of K_2HPO_4, the well-discussed non-Nernstian band-edge-shift mechanism to explain enhanced H_2 production over semiconductor photocatalysts seems not to be applicable to the present case.[10] Excluding the possibility of the photodecomposition of HPO_4^{2-} to H_2 (see Figure S13) and an influence from interface interaction between CN-NS and K_2HPO_4 (see Figure S14), we therefore speculate that the HPO_4^{2-} environment may exert a direct influence on the surface redox reaction. (Photo)electrocatalytic analysis was employed to investigate the origin of the markedly enhanced H_2-evolution performance with HPO_4^{2-}.[10b] Generally, semiconductor photocatalytic H_2 evolution is considered to occur on the surface of loaded cocatalysts (Pt in this case) by proton reduction (see Figure S15).[13] Therefore, by using Pt as the working electrode, we first examined linear sweep voltammetry (LSV) of the electrocatalytic H_2 evolution to simulate the proton-reduction pathway on platinum-loaded CN-NS during the photocatalysis. As shown in Figure 3 a, a reduction current with an onset at nearly 0 V (versus a reversible hydrogen electrode (RHE)) was observed, thus indicating that the H_2-evolution reaction occurred on the Pt surface.[14] Furthermore, when the amount of K_2HPO_4 added was increased from 0 to 0.20 mol, the current density increased by a factor of more than 10 at 0.3 V, thus suggesting that added K_2HPO_4 is capable of effectively promoting H_2 evolution on the Pt surface. To rule out an effect of the pH value, experiments were also performed at the same pH value of 10.14 with different amounts of K_2HPO_4, and consistent results were also obtained (see Figure S16). According to a report by Kreuer and co-workers, such a promotion in H_2 evolution might be partly attributed to the increased proton conductivity: the addition of HPO_4^{2-} can

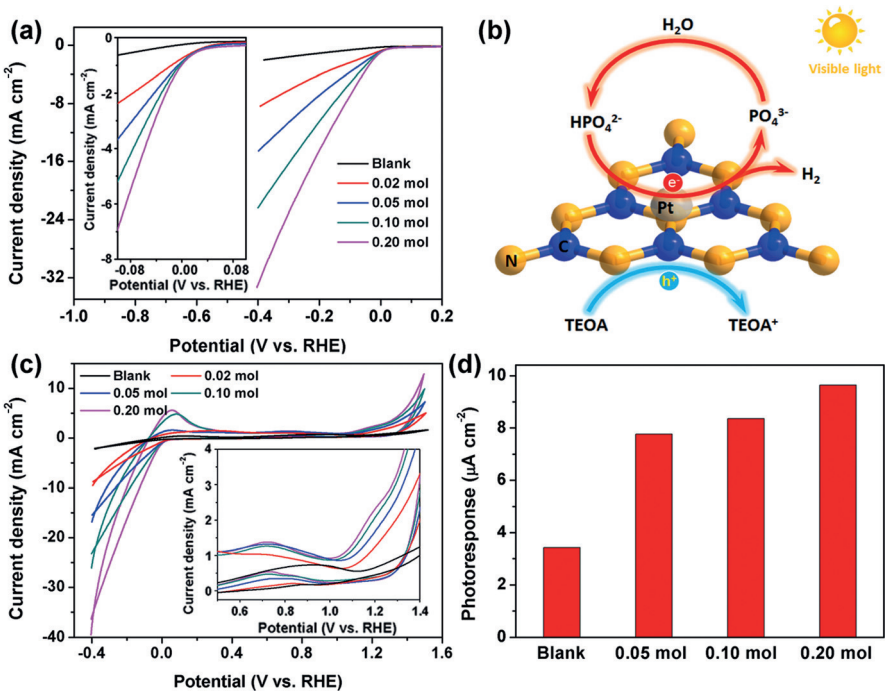

Figure 3. a) Electrochemical H_2 evolution on Pt electrodes in electrolytes containing different amounts of K_2HPO_4. The inset shows the enlarged LSV curves in the potential range of −0.1 to 0.1 V. b) Schematic illustration of photocatalytic H_2 evolution under the proposed proton-reduction mechanism involving HPO_4^{2-}. c) Voltammograms obtained at Pt electrodes for TEOA solutions with and without K_2HPO_4. The inset shows the TEOA-oxidation peaks. d) Net oxidation photocurrent density for TEOA on CN-NS electrodes with different amounts of K_2HPO_4. (The net photoresponse in this case was obtained by subtracting the dark current from the total photocurrent. Visible-light source: 500 W xenon lamp equipped with an L40 cutoff filter.)

lead to the formation of hydrogen-bonded chains of HPO_4^{2-}, which can function like the proton pump in natural photosynthesis to facilitate proton transport in the reaction solution.[15]

Free-energy diagrams calculated for H_2 evolution from H_2O and HPO_4^{2-} (see Figure S17) clearly showed that HPO_4^{2-} is much more advantageous for the creation of H_2, as evidenced by the larger decrease in free energy than with H_2O. LSV also showed that the addition of HPO_4^{2-} leads to a more positive onset potential for H_2 evolution (see Figure S18). These results imply that, apart from serving as a carrier of protons to facilitate H_2 evolution, HPO_4^{2-} is also likely to be a mediator that participates directly in the photocatalytic reaction, thus giving rise to a new proton-reduction pathway (Figure 3b): HPO_4^{2-} instead of H_2O provides the H^+ to react with photogenerated electrons and subsequently produce H_2 and PO_4^{3-} on the surface of Pt cocatalysts (see Figure S15).[13] As demonstrated by the energy calculations and LSV results, this process is more effective than direct H_2 evolution from H_2O, thus possibly making an additional contribution to the enhancement of photocatalytic efficiency. Because the solution pH values were found to be slightly decreased after the photocatalytic reaction (see Figure S19), it could be speculated that after H_2 evolution from HPO_4^{2-}, the formed PO_4^{3-} immediately combined with H^+ from H_2O to regenerate HPO_4^{2-} and finally complete the proton-reduction cycle (Figure 3b). Clearly, this process show many similarities to the Calvin cycle in natural photosynthesis for carbon fixation.

The influence of adding K_2HPO_4 on TEOA oxidation was investigated by voltammetry. An irreversible oxidation peak was observed at 0.97 V (vs. RHE; see Figure S20a), which could be associated with the oxidation of TEOA.[16] Importantly, as the amount of K_2HPO_4 added increased, the oxidation current density increased, the peak gradually shifted to a more negative potential (0.72 V), and a second oxidation peak appeared at 1.2 V (Figure 3c; see also Figure S21).[16b] These results suggest that the oxidation of TEOA can be promoted efficiently by K_2HPO_4. To better simulate the oxidation reaction occurring in the photocatalytic system, we prepared CN-NS thin films and used them as working electrodes in these photoelectrocatalytic TEOA-oxidation tests (see Figure S22). The net oxidation photocurrent density of TEOA with different amounts of K_2HPO_4 is shown in Figure 3d. It is apparent that the photocurrent density increases as the amount of K_2HPO_4 increases, thus proving that, in the presence of K_2HPO_4, the oxidation of TEOA by the photoexcitation of CN-NS can also be enhanced. This feature would be beneficial for the fast consumption of holes in excited CN-NS and the suppression of e^-/h^+ recombination and should consequent improve the photocatalytic efficiency. We therefore propose that the substantial improvement in photocatalytic H_2 generation over CN-NS might be a result of the synergy of enhanced proton reduction and improved TEOA photooxidation in the presence of HPO_4^{2-}.

In summary, we have demonstrated that an environmental modulation inspired by a natural photosystem, namely, the use of a phosphate environment (precisely, the presence of HPO_4^{2-} ions) can lead to a significant enhancement in photocatalytic H_2 production over CN-NS under visible light. For example, with the optimal addition of HPO_4^{2-}, a high H_2 evolution rate of 947 μmol h^{-1} was observed, with an apparent quantum yield of approximately 26.1% at (420 ± 14.5) nm: the highest value reported for a carbon nitride photocatalyst. This improvement relies on the synergy of enhanced proton reduction and improved TEOA photooxidation, as evidenced by (photo)electrocatalytic analysis and theoretical calculations. As a mimic of natural photosynthesis, this strategy of environmental "phosphorylation" could potentially be applied to other semiconductor systems (see Figure S7) and provide a facile approach to efficient photo-

catalysis, such as H_2 production, CO_2 photoreduction, and photoelectric conversion.

Acknowledgements

This research received financial support from the World Premier International Research Center Initiative (WPI Initiative) on Materials Nanoarchitectonics (MANA), MEXT (Japan), and the National Basic Research Program of China (973 Program, 2014CB239301).

Keywords: energy conversion · graphitic carbon nitride · hydrogen production · photocatalysis · photosynthesis

How to cite: *Angew. Chem. Int. Ed.* **2015**, *54*, 13561 – 13565
Angew. Chem. **2015**, *127*, 13765 – 13769

[1] a) A. Kudo, Y. Miseki, *Chem. Soc. Rev.* **2009**, *38*, 253; b) N. S. Lewis, D. G. Nocera, *Proc. Natl. Acad. Sci. USA* **2006**, *103*, 15729; c) J. A. Turner, *Science* **2004**, *305*, 972; d) F. E. Osterloh, *Chem. Soc. Rev.* **2013**, *42*, 2294; e) U. Eberle, M. Felderhoff, F. Schüth, *Angew. Chem. Int. Ed.* **2009**, *48*, 6608; *Angew. Chem.* **2009**, *121*, 6732; f) H. Tong, S. Ouyang, Y. Bi, N. Umezawa, M. Oshikiri, J. Ye, *Adv. Mater.* **2012**, *24*, 229; g) Z. Zou, J. Ye, K. Sayama, H. Arakawa, *Nature* **2001**, *414*, 625.

[2] a) S. Cao, J. Low, J. Yu, M. Jaroniec, *Adv. Mater.* **2015**, *27*, 2150; b) X. Wang, K. Maeda, A. Thomas, K. Takanabe, G. Xin, J. M. Carlsson, K. Domen, M. Antonietti, *Nat. Mater.* **2009**, *8*, 76; c) V. W.-h. Lau, M. B. Mesch, V. Duppel, V. Blum, J. Senker, B. V. Lotsch, *J. Am. Chem. Soc.* **2015**, *137*, 1064; d) S. Yang, Y. Gong, J. Zhang, L. Zhan, L. Ma, Z. Fang, R. Vajtai, X. Wang, P. M. Ajayan, *Adv. Mater.* **2013**, *25*, 2452; e) J. Zhang, M. Zhang, C. Yang, X. Wang, *Adv. Mater.* **2014**, *26*, 4121; f) M. K. Bhunia, K. Yamauchi, K. Takanabe, *Angew. Chem. Int. Ed.* **2014**, *53*, 11001; *Angew. Chem.* **2014**, *126*, 11181; g) C. A. Caputo, M. A. Gross, V. W. Lau, C. Cavazza, B. V. Lotsch, E. Reisner, *Angew. Chem. Int. Ed.* **2014**, *53*, 11538; *Angew. Chem.* **2014**, *126*, 11722; h) Y. Zheng, L. Lin, X. Ye, F. Guo, X. Wang, *Angew. Chem. Int. Ed.* **2014**, *53*, 11926; *Angew. Chem.* **2014**, *126*, 12120; i) Y.-S. Jun, J. Park, S. U. Lee, A. Thomas, W. H. Hong, G. D. Stucky, *Angew. Chem. Int. Ed.* **2013**, *52*, 11083; *Angew. Chem.* **2013**, *125*, 11289; j) D. J. Martin, K. Qiu, S. A. Shevlin, A. D. Handoko, X. Chen, Z. Guo, J. Tang, *Angew. Chem. Int. Ed.* **2014**, *53*, 9240; *Angew. Chem.* **2014**, *126*, 9394; k) K. Schwinghammer, M. B. Mesch, V. Duppel, C. Ziegler, J. Senker, B. V. Lotsch, *J. Am. Chem. Soc.* **2014**, *136*, 1730; l) J. V. Liebig, *Ann. Pharm.* **1834**, *10*, 10; m) Y. Wang, X. Wang, M. Antonietti, *Angew. Chem. Int. Ed.* **2012**, *51*, 68; *Angew. Chem.* **2012**, *124*, 70.

[3] a) P. Niu, L. Zhang, G. Liu, H.-M. Cheng, *Adv. Funct. Mater.* **2012**, *22*, 4763; b) Y. Zhang, A. Thomas, M. Antonietti, X. Wang, *J. Am. Chem. Soc.* **2009**, *131*, 50.

[4] M. Zhang, X. Wang, *Energy Environ. Sci.* **2014**, *7*, 1902.

[5] a) Y. Zhang, T. Mori, J. Ye, M. Antonietti, *J. Am. Chem. Soc.* **2010**, *132*, 6294; b) X. Chen, J. Zhang, X. Fu, M. Antonietti, X. Wang, *J. Am. Chem. Soc.* **2009**, *131*, 11658.

[6] a) T. Sano, S. Tsutsui, K. Koike, T. Hirakawa, Y. Teramoto, N. Negishi, K. Takeuchi, *J. Mater. Chem. A* **2013**, *1*, 6489; b) X. Zhang, X. Xie, H. Wang, J. Zhang, B. Pan, Y. Xie, *J. Am. Chem. Soc.* **2013**, *135*, 18.

[7] a) N. A. Campbell, J. B. Reece, L. A. Urry, M. L. Cain, S. A. Wasserman, P. V. Minorsky, R. B. Jackson, *Biology*, 8th ed., Pearson Benjamin Cummings, San Francisco, CA, **2008**, pp. 162 – 203; b) N. Sato, *J. Plant Res.* **2004**, *117*, 495; c) P. Mitchell, J. Moyle, *Nature* **1967**, *213*, 137; d) F. H. Westheimer, *Science* **1987**, *235*, 1173; e) J. Heberle, J. Riesle, G. Thiedemann, D. Oesterhelt, N. A. Dencher, *Nature* **1994**, *370*, 379.

[8] X. Lu, K. Xu, P. Chen, K. Jia, S. Liu, C. Wu, *J. Mater. Chem. A* **2014**, *2*, 18924.

[9] H. Xu, J. Yan, X. She, L. Xu, J. Xia, Y. Xu, Y. Song, L. Huang, H. Li, *Nanoscale* **2014**, *6*, 1406.

[10] a) P. Wu, J. Wang, J. Zhao, L. Guo, F. E. Osterloh, *Chem. Commun.* **2014**, *50*, 15521; b) S. Ouyang, H. Tong, N. Umezawa, J. Cao, P. Li, Y. Bi, Y. Zhang, J. Ye, *J. Am. Chem. Soc.* **2012**, *134*, 1974; c) T. Simon, N. Bouchonville, M. J. Berr, A. Vaneski, A. Adrović, D. Volbers, R. Wyrwich, M. Döblinger, A. S. Susha, A. L. Rogach, F. Jäckel, J. K. Stolarczyk, J. Feldmann, *Nat. Mater.* **2014**, *13*, 1013.

[11] Y. Kwon, S. C. S. Lai, P. Rodriguez, M. T. M. Koper, *J. Am. Chem. Soc.* **2011**, *133*, 6914.

[12] F. Wang, Y. Jiang, A. Gautam, Y. Li, R. Amal, *ACS Catal.* **2014**, *4*, 1451.

[13] J. Yang, D. Wang, H. Han, C. Li, *Acc. Chem. Res.* **2013**, *46*, 1900.

[14] J. Luo, J.-H. Im, M. T. Mayer, M. Schreier, M. K. Nazeeruddin, N.-G. Park, S. D. Tilley, H. J. Fan, M. Grätzel, *Science* **2014**, *345*, 1593.

[15] L. Vilčiauskas, M. E. Tuckerman, G. Bester, S. J. Paddison, K.-D. Kreuer, *Nat. Chem.* **2012**, *4*, 461.

[16] a) L. Zheng, Y. Chi, Y. Dong, L. Zhang, G. Chen, *J. Phys. Chem. C* **2008**, *112*, 15570; b) S. Karastogianni, S. Girousi, *Sens. Electroanal.* **2014**, *8*, 241.

Received: June 24, 2015
Revised: August 15, 2015
Published online: September 21, 2015

